

# Fatigue Crack Propagation in BFRP Reinforced RC Beams Based on Fracture Mechanics and Golden Ratio

Jun Song, Jian-ting Zhou, Rui Jiang, Ming-bin Wang, Xiao Yu, Shao-li Jia, Fuyan Chen

**Abstract**—The influence of fiber orientation on crack propagation has been studied with BFRP reinforced RC beams. Fracture mechanics parameters were calculated by FEM based on anisotropic elasticity, and the golden ratio which has always been regarded as a model of beauty, for its geometric shape and properties and wide application of painting, sculpture, music, art and architectural. The proportion of the shape is quite beautiful, and BFEP developed rapidly in China with a large number of steel reinforcements in concrete bridges. In this paper, it is first introduced to evaluate the crack distribution pattern of RC beams strengthened with BFRP in the golden ratio. A simulation based on a single reinforcement tension model which can predict the crack width and spacing, combined with an experimental and numerical scale model of reinforcement will prove the accuracy of the parameters. The results show that the golden ratio can analyze the cracks of RC beams strengthened with BFRP, and the cracking model has a physical significance. The results also reveal the existence of a size effect in RC beams, including crack propagation under mixed loading. All the data tend to merge a single relationship when correlated to total energy-release-rate range divided by Young's modulus.

**Keywords**—Golden ratio, model experiment, geometry, crack mode

## I. INTRODUCTION

THE fiber orientation produced by injection molding has a large influence on the propagation rate and path of fatigue cracks [1]. The crack propagation rate perpendicular to aligned fibers is much slower than that parallel to fibers when compared with the same stress intensity range. Novak [3] proposed the range of the energy release rate as a fracture mechanics parameter which gave a unique relation irrespective of fiber orientation. Akiniwa [4] proposed to use the stress intensity range divided by Young's modulus as a controlling parameter for crack propagation with different orientations. In our previous works [5], we also found that the relationship between the crack propagation rate and the stress

intensity range divided by Young's modulus are unrelated to fiber orientation. The effect of R ratio on fatigue crack propagation rate became minimal when correlated to the range of energy release rate divided by Young's modulus [11]. The macroscopic as well as microscopic path of crack propagation was influenced by the fiber orientation, and cracks often propagated under a mixed mode condition even if the applied load was uniaxial.

The classical theory of cracking in RC structures is based on the evaluation of the transfer length ( $l_{tr}$ ), which is the distance between a crack and the nearest cross section having no slip between steel and concrete. The maximum stress of concrete in tension can be detected in this cross section, where a new crack is likely to develop. As a consequence, in RC ties or beams, the crack spacing  $S_r$  lies within the range  $l_{tr} < S_r < 2l_{tr}$  [1]. Both  $l_{tr}$  and  $S_r$  are needed to compute the crack width ( $w$ ) [2-4] generally considered as the difference between the extension of the reinforcement over the crack spacing and the extension of concrete between the cracks. Borosnyoi and Balazs [2] used more than 20 formulas for the calculation of crack distance. It can be considered, for instance, the bond-slip relationship used to model the interaction between steel and concrete. This interaction is influenced by numerous parameters, which are not effectively considered by the model proposed by Ciampi [5].

In particular, the ancient Greek Euclid [3] is the first to propose the "golden ratio", and the third definition states that a straight line is said to have been cut in extreme and mean ratio when, as the whole line is to the greater segment, so is the greater to the less. In other words, in the line segment depicted in Fig. 1, it is possible to localize a point where the ratio of the whole line (A) to the large segment (B) is the same as the ratio of the large segment (B) to the small one (C). It is there that the ratio is equal to the golden ratio, thus arriving at Equation (1).

$$\frac{C}{B} = \frac{B}{A} = \phi = \frac{\sqrt{5}-1}{2} = 0.61803... \quad (1)$$

In mathematics, and this number is interconnected with the Fibonacci sequence (1,2,3,5,8,13,21,...). The ratio of the two digits  $2/3, 3/5, 5/8, 8/13, 13/21, ...$  is what controls growth in Nature. Precisely, the limit of the ratios of two successive terms of the series tends toward the golden ratio.

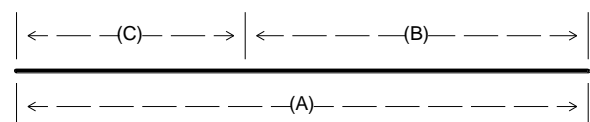


Fig. 1. Line segment divided in accordance with the golden ratio

Manuscript received Nov 30, 2015; revised Oct 7, 2016. This work was supported by the National Natural Science Foundation (551508261/E080505) and the Fund of National Engineering and Research Center for Mountainous Highways (No. GSGZJ-2014-03).

Jun Song is with the School of Civil Engineering, University of LuDong, Yantai, CHINA (corresponding author to provide phone: 13021617898; e-mail: songjun198298@163.com).

Jian-ting Zhou was with the School of Civil Engineering & Architecture University of Chongqing Jiaotong, Chongqing, CHINA. (e-mail: jt-zhou@163.com).

Rui Jiang is with the School of Civil Engineering, University of LuDong, Yantai, CHINA (e-mail: Jiangrui@yahoo.cn).

Although the golden ratio is applied in many subjects [10-15], the basic application of its geometric properties, lacks structural mechanics problems in depth analysis. Moorman [8] analyzed the classical coupled oscillation problem with the golden ratio. Zhi-Jian [9] studied the elastic plastic problem of crack plate with the golden ratio. These studies have played a key role in the understanding and application of the golden ratio.

In this paper, we analyze the crack patterns of basalt fiber [16-17] reinforced concrete beams by using the golden section ratio and then use the "single rib tensile model" to establish the balance equation.

## II. CRACKING MODEL FOR RC BEAM

In order to calculate the crack patterns of the basalt strengthened beams, the crack patterns of ordinary reinforced concrete beams are firstly established.

Figure 2 shows the distribution of crack analysis calculation model to inverse the single beam flexural cracks. The tensile test model of the reinforced concrete beam (see Fig.2) can be used to reveal the cracking phenomenon, and when the normal load reaches the cracking load, cracks will appear in the position of  $L-2l_{tr}$ , and at this time the concrete stress is utilized to achieve the design of a tensile load.

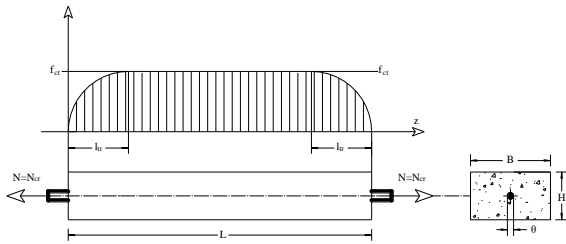


Fig. 2 The stress distribution of the single bar in the horizontal force

The development of cracks is random, and here two cases of the crack mode and distribution are shown in Fig.3 and Fig.4. If an axial force N is given, and the strain of the reinforcement  $\epsilon_s$ , strain of concrete  $\epsilon_c$ , then the Equation (2) can be obtained as follows:

$$N = \sigma_s A_s + \sigma_c A_c = E_s \epsilon_s A_s + E_c \epsilon_c A_c \quad (2)$$

$A_s$  stands for the area of rebar,  $A_c$  stands for the area of concrete,  $E_c, E_s$  stands for the elastic modulus of concrete and reinforced concrete.

The strain and concrete strain can be obtained by Equation (2).

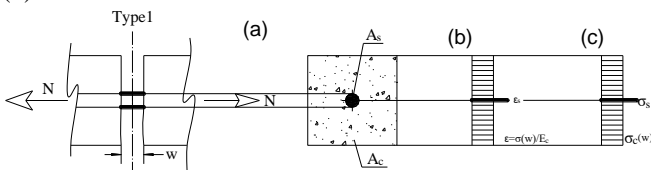


Fig. 3(a) Geometrical properties of Type1 (b)strain(c)stress

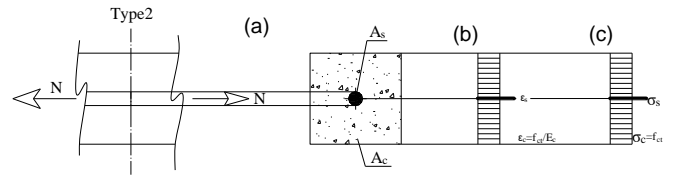


Fig. 4 (a) Geometrical properties of Type2 (b)strain(c)stress

Considering the maximum cracking width in the reinforced concrete beams, and the loading process is assumed to be consistent with the assumption of plane cross section. Then the maximum crack spacing will be changed, and the rule of change is about equal to half of the new cracking space. The early formation of the new crack pattern, as shown above, in this case will be the new crack section when the ultimate tensile stress occurs.

## III. PROGRAM CALCULATION

According to Fig.3 and Fig.4 presents the Type 1 and Type 2 types of construction, and the construction calculation diagram is shown in Fig.5. In the Type1 section, when  $z=0$ ,  $s(z=0) = w/2$ . In the Type 2 section, when  $z=l_{tr}$ ,  $\sigma_c(z=l_{tr}) = f_{ct}$ . The calculation procedures are as follows:

- ① Assuming a crack width values;
- ② Assuming an experimental load value of tensile reinforcement;
- ③ The normal stress of Type 1 section is calculated;
- ④ In the calculation mode of the Type 2 section, and the strain of the steel bar in the initial crack can be obtained.;
- ⑤ Assuming a cracking transfer length  $l_{tr}$ , divide into N parts, so the length of each section is  $\Delta z = l_{tr} / n$ ;
- ⑥ Because the static and dynamic relations are known, the numerical integration can be solved by the formula (3), It is assumed that the increment of the strain of the steel bar and concrete strain increment are the same:

$$\begin{aligned} \epsilon_{s,i} &= \epsilon_{s,0} - \chi_i (\epsilon_{s,0} - \epsilon_{s,n}) \\ \epsilon_{c,i} &= \epsilon_{c,0} - \chi_i (\epsilon_{c,0} - \epsilon_{c,n}) \end{aligned} \quad (3)$$

$\epsilon_{c,n}, \epsilon_{s,n}$  Represent the strain values of concrete and reinforced concrete and steel in the Type 2,  $\epsilon_{c,0}, \epsilon_{s,0}$  stands for the strain values of concrete and reinforced concrete and steel in the Type 1., and  $0 \leq \chi_i \leq 1$ .

$$s_i = s_{i-1} - \Delta z \left[ -\chi_i (s_{s,0} - s_{s,n} + s_{c,0} - s_{c,n}) + s_{s,0} - s_{c,0} \right] \quad (4)$$

The finite difference method is used to calculate the strain value  $\epsilon_{s,i}$  of the reinforcement with Equation (5).

$$\epsilon_{s,i} = \epsilon_{s,i-1} - \Delta z \frac{4}{\phi E_s} \tau_{i-1} \quad (5)$$

- ⑦ If at nth point,  $s_n \neq 0$ , change  $l_{tr}$  and go back to Step ⑥;
- ⑧ If at nth point,  $\epsilon_{s,n} \neq f_{ct} / E_c$ , and  $\chi_i \neq 1$ , then change  $\epsilon_{s,0}$  and go back to Step ②.

For a given value of crack width  $w$ , the previous procedure provides not only the corresponding normal force  $N$ , but also the maximum distance between the cracks,  $s_{r,max} = 2l_r$ .

IV. MODEL APPLICATION

The proposed model can be used to predict the crack pattern, both in terms of crack spacing and crack width, in RC elements under tensile loads. Specifically, the geometrical properties of the specimens tested by Mitchell are scaled here at a factor  $\alpha$ . When  $\alpha=1$ , the formation of the maximum crack width experimentally measured at various values of applied load  $N$  is depicted in Fig. 5(a).

In this paper, the computational model and Mitch model are compared and analyzed, and the validity of the program is verified, showing that the method can effectively predict the crack width of reinforced concrete beams. As shown in Fig. 6, the relationship between the length of the crack and the stress of the reinforcement is calculated, and the length of the crack is decreased gradually with the increase in the stress level. When the stress reaches the yield stress, when  $\alpha=1$  and  $\alpha=2$ , the result is very close to the golden ratio, as expressed in Formula 6. Therefore, the crack distribution patterns of the reinforced concrete beams can be expressed by the gold partition rate.

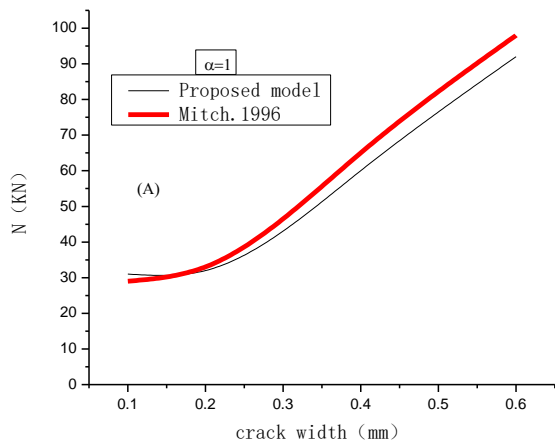


Fig.5 Compared with the Mitch model

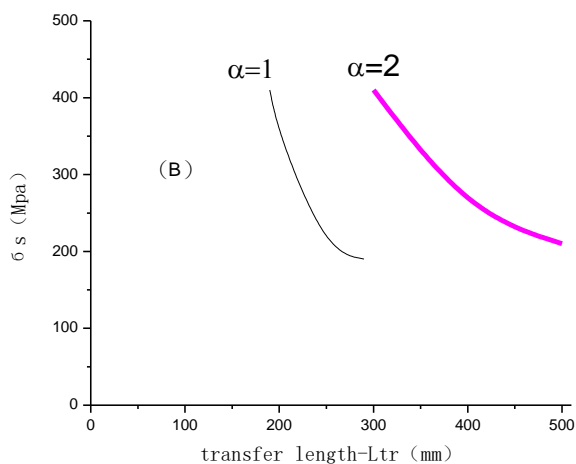


Fig.6 Values of transfer length when  $\alpha=1$  and  $\alpha=2$

$$\left[ \frac{l_r(\alpha=1)}{l_r(\alpha=2)} \right]_{\sigma_s=400Mpa} = \frac{189mm}{308mm} \approx \phi \quad (6)$$

From the above analysis, the crack distribution pattern of the reinforced concrete beam can be determined, and can be used to explain the golden ratio. The transfer length of the crack will be increased with time when the geometrical size of the beam is multiple.

V. PRACTICAL ASSESSMENT OF CRACK SPACING WITH BFRP STRENGTHENED RC BEAM BRIDGE THROUGH A SIZE-EFFECT LAW BASED ON THE GOLDEN RATIO

A. Size Effect Model

The crack spacing can be expressed by the size effect with the multiple variations of the geometrical dimensions. The foreign scholars [10] have done the related research as expressed in a power function. The formula is as follows:

$$\frac{s_{r0}}{s_r} = \left( \frac{D_0}{D} \right)^\mu$$

$D_0$  is the reference size ( $\alpha=1$ ),  $D$  is on behalf of the general scale ( $\alpha>1$ ),  $s_{r0}$  stands for when  $\alpha=1$ , crack space,  $s_r$  stands for when  $\alpha>1$  crack space.  $\mu$  Values can be obtained by model experiments or numerical simulations.

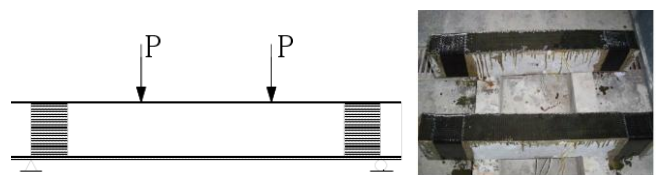


Fig.7 Reinforcement method with BFRP

B. Experiment and Numerical Simulation

In order to calculate  $\mu$  values, this study designs three sets of reinforced concrete beams with BFRP. The experimental beam reinforcement method is used according to the similarity principle [7] the ratio of the three pieces of the experimental beam. Respectively, the sizes which are 900mm, 600mm and 300mm are used. The cross section of the different sized beams is shown in Fig.7, and four point bending test was used in the loading mode, as shown in Fig.7.



Fig.8 Crack distribution of No.1 beam

In the process of the experiment, the crack width, crack spacing, strain, load size and other parameters of the three groups were recorded respectively. Fig.9 shows the crack distribution and extension of the experimental beams. In order to verify the reliability of the model experiment, the failure process of the three experimental beams strengthened was simulated by the large general purpose finite element software ABAQUS. The numerical simulation of the parameters is consistent with the model. The finite element numerical results of the three pieces of reinforced beams are shown in Fig.9.

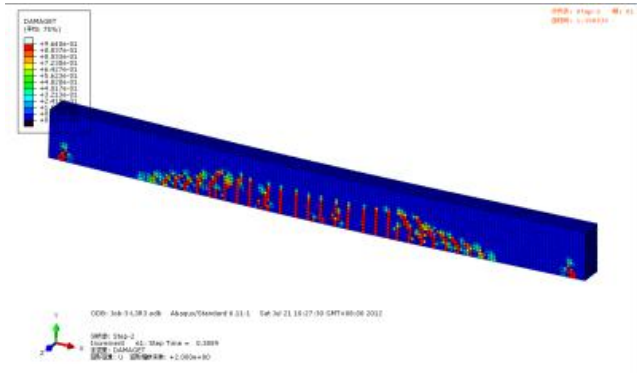


Fig.9 Numerical simulation of the crack distribution

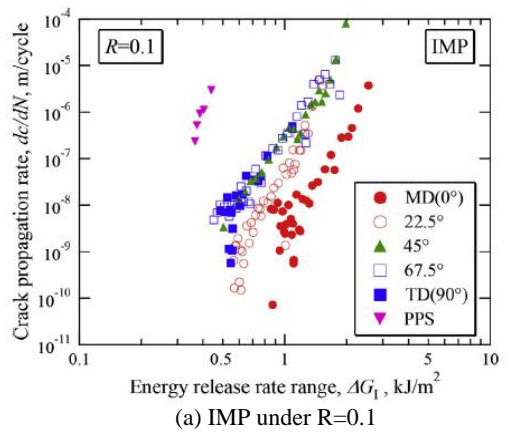
The following conclusion was obtained by using the model experiment and numerical simulation. When the ratio of the geometric dimensions of the beams with BFRP reached  $D_0/D=0.3$ , the fracture propagation length was in accordance with the characteristics of the golden ratio, thus obtaining  $\mu \cong 0.4$ .

In a word, the crack spacing exist size effect can be easily studied in the fracture mode. At the same time, the results can predict the cracks distribution of BFRP reinforcement of the bridge through the reduced scale model.

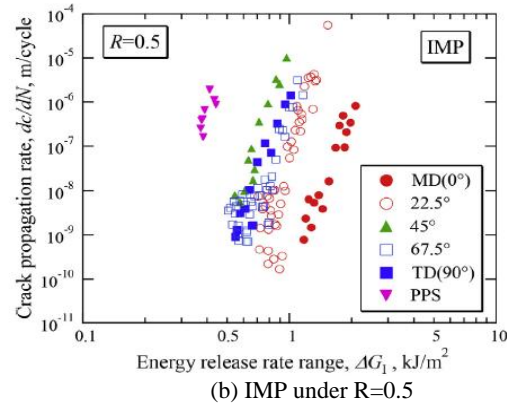
### VI. FATIGUE CRACK PROPAGATION TESTS

Fatigue crack propagation tests [18-22] were performed with a tension-compression electro-servo-hydraulic testing machine. Fatigue testing was done at room temperature under load-controlled conditions with the stress ratio  $R$  of 0.1 and 0.5 for IMP, and 0.1 for SLP. The waveform of the cyclic load was triangular and the frequency was between 2.5 and 8 Hz to maintain a strain rate.

The fatigue crack propagation rate,  $dc/dN$ , for MD and TD specimens of IMP is plotted against the range of mode I stress intensity factor,  $\Delta K_I$ , as shown in Fig.10. There is a linear relation between  $dc/dN$  and  $\Delta K_I$  in log-log diagram. For both cases of  $R = 0.1$  and  $0.5$ ,  $dc/dN$  is the highest in PPS and the lower in MD than in TD. The resistance to crack propagation is improved by fiber reinforcement, and fibers aligned perpendicular to the crack growth direction block more severe crack propagation. For each material,  $dc/dN$  is higher under the larger  $R$  ratio.

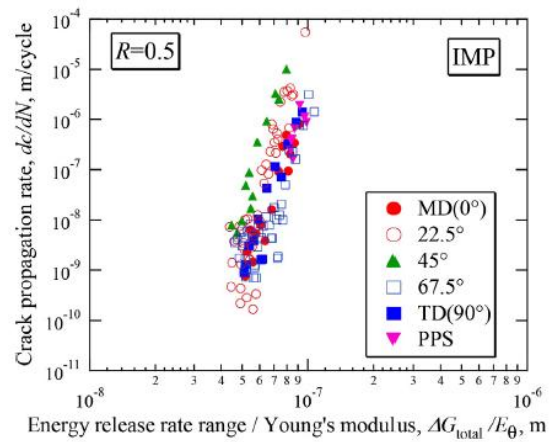


(a) IMP under  $R=0.1$

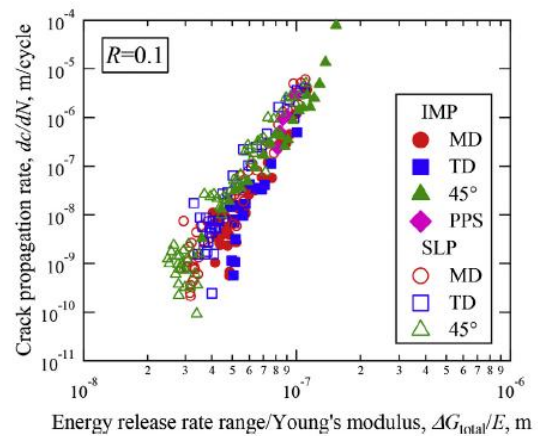


(b) IMP under  $R=0.5$

Fig.10 Crack propagation rate correlated to the ranges of stress intensity factor and energy release rate for IMP



(a) IMP under  $R=0.1$

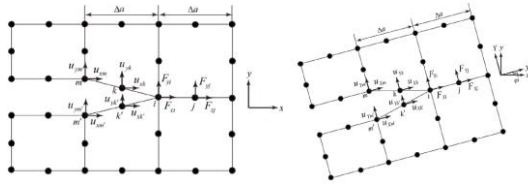


(b) SLP and IMP under  $R=0.5$

Fig.11 Crack propagation rate correlated to the total energy release rate divided by Young's modulus

A. Fatigue crack propagation path

For the crack shown in Fig.12(a) under modes I and II, the energy release rates for mode I is calculated from reactions  $F_{yi}$  and  $F_{yj}$  at nodes i and j ahead of the crack tip, and the upper and lower displacements,  $u_{yk}$  and  $u_{yk0}$ , at node k behind the crack-tip and  $u_{ym}$  and  $u_{ym0}$ , at node m as



(a) Crack under mode I and II (b) Inclined crack under modes I and II

Fig. 12. Forces and displacements near crack tip for MCCI method.

In order to avoid the mesh-size dependency of the calculated values, when the crack is inclined to the direction perpendicular to the loading axis by angle  $\phi$  as shown in Fig.12(b), modes I and II energy release rates can be calculated after converting the reaction and displacement from x-y coordinates to X-Y coordinates, and the above equations are used for X-Y coordinates.

Fig.13(a) shows the change in the correction factor, FI, of mode I stress intensity factor as a function of crack length relative to the specimen width W for MD, TD and isotropic material, ISO. Fig.13(b) shows the ratio of the factor of MD and TD relative to that of ISO. MD has a larger  $F_I$  value than ISO, and TD has a smaller value. The difference is as high as 15%. SLP has a larger difference than IMP, because the degree of anisotropy is larger for SLP.

The change in the correction factor, YI, for mode I energy release rate with relative crack length is shown in Fig.14 for IMP and SLP. The fiber angle, crack angle and degree of anisotropy all have an influence. The YI value is the largest for TD of SLP, and decreases with increasing crack propagation angle  $\phi$  to  $30^\circ$ .

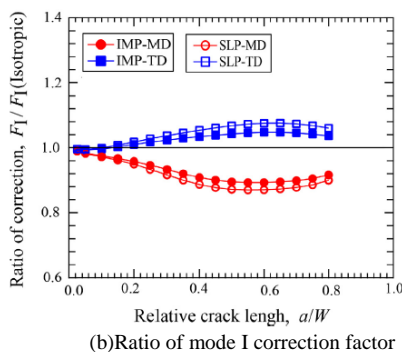
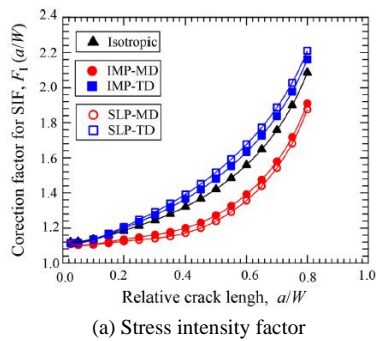


Fig.13 Change in correction factor of mode I stress intensity factor with crack length.

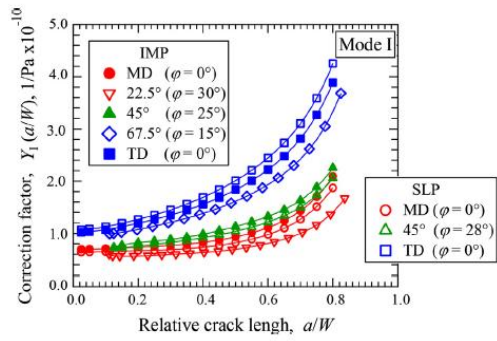


Fig. 14. Change in correction factor of mode I energy release rate with crack length.

VII. CONCLUSIONS

A new method for evaluating the distribution patterns of cracks in reinforced concrete beam bridges with BFRP has been studied. The size effect law of crack spacing can be obtained by using a nonlinear numerical model. The following conclusions can be obtained by combining experimental data and numerical simulation:

- 1) The cracking model of the BFRP beams can be expressed by the golden ratio, and the crack propagation length  $l_{tr}$  of the BFRP beams have the size effect.
- 2) When the ratio of the geometric dimensions of the beams with BFRP reach  $D_0/D=0.3$ , the fracture propagation length is in accordance with the characteristics of the golden ratio. Therefore it can be obtained  $\mu \cong 0.4$ , and the formula can be applied, such as,  $\frac{s_{r0}}{s_r} = \left(\frac{D_0}{D}\right)^\mu$ . The crack distribution of reinforced concrete beam strengthened with BFRP is predicted by the experimental model and numerical simulation.
- 3) Fatigue cracks were propagated under a mixed loading of modes I and II for the fiber angles other than  $0^\circ$  and  $90^\circ$ . The data of the crack propagation rate correlated to the range of total energy release rate.
- 4) All the data of  $dc/dN$  for various fiber angles and R ratios tend to merge a single relation when the rate is correlated to the range of total energy release rate divided by Young's modulus

ACKNOWLEDGEMENTS

This work was supported by the National Natural Science Foundation (51508261/E080505), the University Science and technology project of Shandong Province (No.J16LG60), the Doctoral Program of Ludong University (No. LY2015021), and the Fund of National Engineering and Research Center for Mountainous Highways (No. GSGZJ-2014-03), the University Science and technology project of Shandong Province (No. J15LG01).

REFERENCES

[1] Fantilli, A. P., Ferretti, D., Iori, I., and Vallini, P.(1998) Flexuraldeformability of reinforced concrete beams. *J. Struct. Eng.*124(9),pp.1041-1049.

- [2] Hejazi, M. (2005) Geometry in nature and Persian architecture. *Build. Environ.*, 40(10), pp.1413-1427.
- [3] Chen Hui. (2011) Research on the gold division in the graphic design. *Hebei Normal University*.
- [4] Bazant, Z. P. (1984). Size effect in blunt fracture: Concrete, rock, metal. *J. Engrg. Mech. Div.*, 110(4), pp.518-535.
- [5] Carpinteri, A., Chiaia, B., and Ferro, G. (1995) Size effects on nominal tensile strength of concrete structures: Multifractality of material ligaments and dimensional transition from order to disorder. *Mater. Struct.*, 28(6), pp.311- 317.
- [6] Beeby, A. W. (2005), The influence of the parameter  $w/\text{reff}$  on crack widths. *Struct. Concr.*, 6(4), pp.155- 165
- [7] Yang Junjie. (2005). Similarity theory and structural model experiment.. Wuhan: *Wuhan University of Technology press*. pp.:10-13.
- [8] Moorman, C. M., and Goff, J. E. (2007). Golden ratio in a coupled oscillator problem. *Eur. J. Phys.* 28(5), pp.897-902.
- [9] Zhi-Jian, Y., Shi-Jie, W., and Xiang-Jian, W. (1997). Precise solutions of elastic-plastic crack line fields for cracked plate loaded by antiplane point forces. *Eng. Fract. Mech.*, 57(1), pp.75-83.
- [10] Burtscher, S. (2004). RILEM TC QFS quasibrittle fracture scaling and size effect-Final report. *Mater. Struct.*, 37(8), pp. 547-568.
- [11] Son Duy Dao, Kazem Abhary, and Romeo Marian. Maximising Performance of Genetic Algorithm Solver in Matlab. *Engineering Letters*, 24:1, pp75-83.
- [12] Lackner, R, and Mang, H. A. (2003a). Scale transition in steel-concrete interaction. I: *Model. J. Eng. Mech* , 129(4), pp. 393-402.
- [13] Lackner, R, and Mang, H. A. (2003a). Scale transition in steel-concrete interaction. I: *Model. J. Eng. Mech* , 129(4), pp. 393-402.
- [14] Lackner, R., and Mang, H. A. (2003b). Scale Transition in steel-concrete interaction. II: *Applications. J. Eng. Mech*, 129(4), pp. 403-413.
- [15] Livio, M.. The golden ratio: The story of phi, the world's most astonishing number, *Broadway Books*, 2002 New York.
- [16] Minelli, F., Tiberti, G., and Plizzari, G. A. (2011) Durability and crack control in FRC RC elements: An experimental study. *Int. RILEM Conf. on Advances in Construction Materials through Science and Engineering*, RILEM, Bagneux, France, pp.435-443
- [17] Mitchell, D., Abrishami, H. H., and Mindess, S. (1996). The effect of steel fibers and epoxy-coated reinforcement on tension stiffening and cracking of reinforced concrete. *ACI Mater. J.*, 93(1), pp. 61-68.
- [18] Zhijie Chen, and Hongguang Ji. Temperature Variation of the Early-age Massive Concrete in Freezing Vertical Shaft Wall. *Engineering Letters*, 24:1, pp24-29.
- [19] L. adacher. (2015) The global optimization of signal settings and traffic assignment combined problem: a comparison between algorithms. *Advances in Transportation Studies an international Journal Section A* 36, pp.37-43.
- [20] V. Ratanavaraha, S. Jomnonkwao. (2015) The efficiency testing of Shoulder Rumble Strips (SRS) on noise for alerting drivers in Thailand: a comparison among three types of SRS. *Advances in Transportation Studies an international Journal Section B.* 36, pp.109-117.
- [21] Zhijie Chen. Temperature Variation of the Early-age Massive Concrete in Freezing Vertical Shaft Wall.
- [22] Supriya M, Sangeeta K, and G K Patra. Trustworthy Cloud Service Provider Selection using Multi Criteria Decision Making Methods. *Engineering Letters*, 24:1, pp.1-10.

Jun Song was born in 1982. And he received the Ph.D. degree in Bridge Engineering from Chongqing Jiaotong University, Chongqing, China in 2014. Currently he is a Lecturer at Lu Dong University. His research interests include bridge health monitoring, and structure security evaluation.